Journal of Hydrology 523 (2015) 231–239

Contents lists available at ScienceDirect

Journal of Hydrology

journal homepage: www.elsevier.com/locate/jhydrol

Calibration of SWAT model for woody plant encroachment using paired experimental watershed data

Lei Qiao *, Chris B. Zou, Rodney E. Will, Elaine Stebler

Department of Natural Resource Ecology and Management, Oklahoma State University, Stillwater, OK 74078, USA

ARTICLE INFO

Article history:
Received 12 December 2014
Received in revised form 22 January 2015
Accepted 24 January 2015
Available online 4 February 2015
This manuscript was handled by Geoff Syme, Editor-in-Chief

Keywords:
Juniper
Water resources
Ecosystem services
Rangeland
Great Plains
Upscaling

SUMMARY

Globally, rangeland has been undergoing a transition from herbaceous dominated grasslands into tree or shrub dominated woodlands with great uncertainty of associated changes in water budget. Previous modeling studies simulated the impact of woody plant encroachment on hydrological processes using models calibrated and constrained primarily by historic streamflow from intermediate sized watersheds. In this study, we calibrated the Soil and Water Assessment Tool (SWAT model), a widely used model for cropping and grazing systems, for a prolifically encroaching juniper species, eastern redcedar (*Juniperus virginiana*), in the south-central Great Plains using species-specific biophysical and hydrological parameters and *in situ* meteorological forcing from three pairs of experimental watersheds (grassland versus eastern redcedar woodland) for a period of 3-years covering a dry-to-wet cycle. The multiple paired watersheds eliminated the potentially confounding edaphic and topographic influences from changes in hydrological processes related to woody encroachment. The SWAT model was optimized with the Shuffled complexes with Principal component analysis (SP-UCI) algorithm developed from the Shuffled Complexes Evolution (SCE_UA). The mean Nash–Sutcliff coefficient (NSCE) values of the calibrated model for daily and monthly runoff from experimental watersheds reached 0.96 and 0.97 for grassland, respectively, and 0.90 and 0.84 for eastern redcedar woodland, respectively. We then validated the calibrated model with a nearby, larger watershed undergoing rapid eastern redcedar encroachment. The NSCE value for monthly streamflow over a period of 22 years was 0.79. We provide detailed biophysical and hydrological parameters for tallgrass prairie under moderate grazing and eastern redcedar, which can be used to calibrate any model for further validation and application by the hydrologic modeling community.

1. Introduction

Woody plant encroachment and expansion into rangeland is widely reported in semi-arid and arid regions of the world (Archer et al., 1995; Schimel et al., 2001; Briggs et al., 2005; Wilcox, 2007; Ratajczak et al., 2011). This physiognomic change could alter rangeland function and services such as the water budget and carbon cycles by changing the atmosphere–ecosystem interaction and feedback as well as the groundwater and surface water interaction (Houghton et al., 1999; Schimel et al., 2001; Huxman et al., 2005). Many studies focused on changes in vegetation phenology, biodiversity, tree–grass interactions, and carbon and nutrient dynamics during the progression of woody plant encroachment (Archer et al., 1988; Briggs and Knapp, 1995; Norris et al., 2001; Ratajczak et al., 2011; O'Donnell and Caylor, 2012). A number of field studies documented that woody plant encroachment alters the water budget, reduces streamflow or groundwater recharge, and impairs water resources availability in semiarid and subhumid regions (Huang et al., 2006; Zou et al., 2013). Improved understanding of such impacts, especially on watershed and river basin scales, is particularly important for guiding global change adaptation practices to sustain the socio-ecological systems in water-limited regions (Dugas et al., 1998; Huxman et al., 2005; Huang et al., 2006; Newman et al., 2006; Owens et al., 2006; Engle et al., 2008; Zou et al., 2013).

In the south-central Great Plains, rangeland has been undergoing a steady transition from herbaceous dominated grassland into a tree or shrub dominated woodland for nearly a century and this transition has been accelerating in the recent decades, primarily due to an evergreen juniper species, eastern redcedar (*Juniperus virginiana*) (Briggs et al., 2005; Engle et al., 2008). The juniper woodland presents 20 times or more aboveground standing biomass in comparison to that of the warm-season grassland at its peak during the growing seasons (Briggs and Knapp, 1995; Norris et al., 2001). The greater accumulation of biomass and litter above-

* Corresponding author. Tel.: +1 (405) 744 9637.
E-mail address: lei.qiao@okstate.edu (L. Qiao).

http://dx.doi.org/10.1016/j.jhydrol.2015.01.056
0022-1694/

ground in redcedar stands result in higher rainfall interception, with as high as 35–37% of total precipitation being intercepted by the juniper canopy and litter layer (Owens et al., 2006). Starks et al. (2014) showed that redcedar canopies could intercept 100% of precipitation for events less than 2.4 mm.

Juniper species are capable of developing much deeper root systems than herbaceous vegetation and can potentially access water deeper in the soil profile (McCole and Stern, 2007). Recent studies reported excessive depletion of rooting zone soil moisture for eastern redcedar woodland in winter and early spring when the warm-season grass is still dormant (Zou et al., 2013; Caterina et al., 2014). Early work on plot-level Bowen ratio-energy balance method in the Edwards Plateau of Texas suggested that the actual evapotranspiration (ET_a) of Ashe juniper (*Juniperus ashei*) (similar to eastern redcedar) woodland was 35–85 mm higher than that of adjacent grassland on annual basis (Dugas et al., 1998). Lately, a few studies have explored the effects of woody encroachment on hydrological properties and therefore streamflow and groundwater recharge on plot or experimental watershed scales (Huang et al., 2006; Zou et al., 2013) and used Landsat 5 remote sensing data for ET_a of Oklahoma (Liu et al., 2010).

Plot scale or experimental watershed observations are critical in understanding the underlying mechanisms of woody encroachment on components of the water cycle, but process-based modeling is more effective to evaluate encroachment impacts for large watersheds with spatial heterogeneity and climate gradients. A few modeling efforts investigated juniper encroachment and brush management on water resources primarily in southern Texas and Arizona (Bednarz et al., 2000; Wu et al., 2001; Brown and Raines, 2002; Afinowicz et al., 2005; Bumgarner and Thompson, 2012; O'Donnell and Caylor, 2012; Pierini et al., 2014). Wu et al. (2001) evaluated rangeland management scenarios and water yield dynamics in the Cusenbary Draw basin (207 km^2) of the Edwards Plateau using the Simulation of Production and Utilization of Rangelands (SPUR-91) model. They estimated that annual water yield increased by as much as 200 mm when woody cover was reduced by 40%. Afinowicz et al. (2005) carried out a similar simulation for the North Fork of the Upper Guadalupe River basin (360 km^2) within the same Edwards Plateau but with SWAT, and predicted ET_a reductions ranging from 31.9 to 46.6 mm y^{-1} after removing juniper. The apparent discrepancy of estimated ET_a from these two modeling studies reflects the challenge in simulating hydrological impacts of woody encroachment, a novel land transformation process, without adequately calibrating and constraining model parameters with observation data.

Since most studies beyond the experimental watershed scale are limited by data availability, usually a single source of streamflow measurement is used for model calibration and validation. This approach is particularly insufficient for woody encroachment as streamflow data capturing this physiognomic transformation is rare (Wine et al., 2011). Moreover, due to the lack of biophysical parameters for juniper in many existing model databases, values for pine species (also evergreen) are commonly used (e.g., Afinowicz et al., 2005; Bumgarner and Thompson, 2012). For juniper species, the biophysiological characteristics such as phenology, average height, rooting depth, foliage architecture and attributes, and stomata conductance could differ greatly from pine species and a proper representation of these parameters in the modeling algorithm is needed. Finally, woody plant encroachment and transition from herbaceous dominated landscape to woody state is associated with a unique suite of changes in soil physical and hydrological properties (Zou et al., 2013). This also needs to be adequately incorporated in the model calibration process.

The objective of this research was to understand how physically based hydrological transport models, such as SWAT, can be improved by using *in situ* observations at the experimental watershed scale for eastern redcedar, a widely encroaching juniper species in the south-central Great Plains. Our specific objectives were: (1) to refine and compile biophysical parameterization of eastern redcedar in the SWAT model using comprehensive *in-situ* observations and measurements, (2) validate the calibrated SWAT model in large (landscape-scale) watersheds to demonstrate its capability in simulating eastern redcedar encroachment impacts on streamflow and groundwater recharge at larger scales. We will discuss the application of improved SWAT model for understanding temporal evapotranspiration dynamics, and interactive effect of climate change and woody plant encroachment on alteration of hydrological cycle at multiple spatial scales.

2. Materials and methods

2.1. Site description and data acquisition

2.1.1. The small-scale experimental watersheds

Six experimental watersheds (three for grassland and three for redcedar encroached grassland) were instrumented in the Cross-timbers Experimental Range of the lower Cimarron River basin of northern Oklahoma in 2010 (Fig. 1a). These experimental watersheds are located close to each other, separated by less than 1 km, and are comparable in size (2–5 ha). The slope of these experimental watersheds ranges from 5% to 7%, with coarser sandy loam soil in the upper slope and finer clay loam soil in the lower slope positions. The underling rock is mainly shale and sand stone.

At the study site, meteorological variables were measured at two weather stations, one located in a grassland experimental watershed and the other in a watershed encroached by eastern redcedar. Variables measured at the stations included air temperature and relative humidity (Vaisala, Helsinki, Finland), wind speed and direction (RM Young Company, Traverse City, MI, USA), solar radiation (Apogee Instruments, Inc., Logan, UT, USA), soil temperature at 5 cm depth (Campbell Scientific, Logan, UT, USA), and precipitation (Hydrological Services America, Lake Worth, FL, USA). The annual precipitation for 2011, 2012 and 2013 was 616, 631, and 979 mm, respectively, which covers a dry-to-wet cycle and includes two extreme dry years in contrast to the long term annual mean precipitation of around 900 mm from the nearby Marena Oklahoma MESONET station. The meteorological forcing of the grassland and eastern redcedar encroached watersheds was similar with minor differences. Primarily, the wind speed was higher in grassland, resulting in higher potential evapotranspiration (PET) than in the eastern redcedar encroached watershed. The soil water storage was quantified with a total of 18 ECH_2O soil moisture arrays (Decagon, Pullman, WA, USA) (three per watershed). Each array had four EC-5 sensors along the soil profile at the depths of 5, 20, 45, and 80 cm. Surface runoff was measured using either a 3 or 4 feet H-flume at the base of each watershed (Zou et al., 2013). Data quality and error control are very important in watershed studies and can be influenced by the streamflow measuring equipment (Harmel et al., 2006). The H-flumes had attached stilling wells with float movement sensed by optical shaft encoders (HydroLynx Systems, Inc., West Sacramento, CA, USA) which continuously recorded stage level via dataloggers (Campbell Scientific, Logan, UT, USA). Construction and installation of the H-flumes and their appropriate concrete approach sections followed recommended specifications and procedures (Holtan et al., 1962) and equations based on the supplied ratings table for the stage-discharge relationship were used to convert stage level to streamflow rate. Calibration of the stage level was checked monthly and reset as needed. Accuracy of the stage readings was periodically verified by measuring stage depth with a ruler during discharge events.

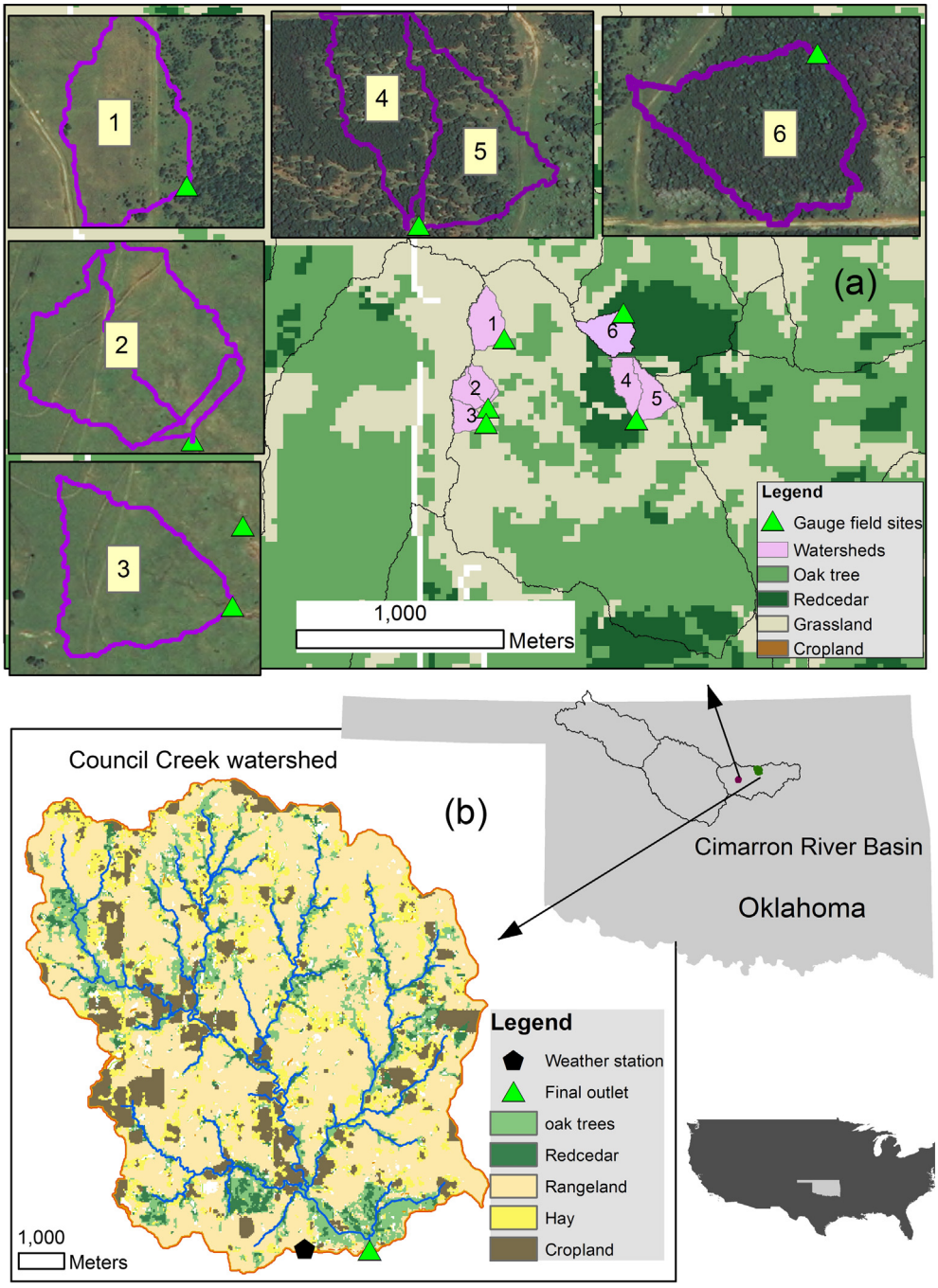

Fig. 1. (a) Land cover and land use by National Land Cover Database (NLCD) 2006 of the paired experimental watersheds for this study. The enlarged aerial photo shows the small-scale watersheds (2–5 ha) with runoff monitoring gauges to measure hydrological responses of grassland (# 1, 2 and 3) and eastern redcedar encroachment (# 4, 5 and 6). (b) The land use and land cover by NLCD 1992 and streamflow network of the Council Creek watershed that was used to validate the SWAT model. Note the spatial scale difference of the experimental watershed and the Council Creek watershed.

2.1.2. The Council Creek watershed

The Council Creek watershed (Fig. 1b), located 30 km away from the experimental watershed sites, was selected as the SWAT validation watershed. This watershed was chosen because eastern redcedar encroachment and forest expansion in the riparian zones of this watershed are representative for the south-central Great Plains (Wine and Zou, 2012). It is an intermediate sized watershed (78 km^2 area) with relatively flat relief which is similar to the experimental watersheds except that the larger spatial scale includes a 68 km long streamflow channel. Soils are medium-textured ranging from 0 to 190 cm in depth although generally less than 100 cm deep in the upland areas (Soil Conservation Service, 1987). Underlying subsurface geology is primarily sedimentary rock of shale and sandstone of Late Pennsylvanian age (Stoeser, 2005).

2.2. SWAT model description and eastern redcedar parameterization

SWAT is a physically based hydrological transport model for small watersheds to river basin-scale simulations. Model outputs include the quality and quantity of surface and ground water and prediction of the environmental impacts of land use, land manage-

ment practices, and climate change (Arnold et al., 1998, 2012). The smallest spatial unit in SWAT is the hydrologic response unit (HRU) featured with unique land cover, soil type, and topographic slope. The Soil Survey Geographic database (SSURGO) and National Land Cover Database (NLCD) 2006 were used to define the HRUs. LiDAR elevation data with resolution of 1.4 m was used to delineate watershed boundaries and the flow routing systems. These are currently the most accurate datasets for the U.S. suitable for the modeling of 2–5 ha watersheds.

A series of representative plant biophysical and hydrological parameters were selected for eastern redcedar and grassland parameterization (Table 1). Mostly, the grass parameters are from the default SWAT database, with minor changes during calibration. We parameterized the eastern redcedar based on our field observations and literature review. Due to variability of tree distribution, density, and growth status, an uncertainty range was given for each parameter.

The maximum canopy storage of precipitation and Leaf Area Index (LAI) determine how much water will be intercepted by the canopy, which further alters ET flux and throughfall amount received at the land surface. Starks et al. (2014) showed that redcedar maximum canopy storage (CANMAX) was about 2.4 mm in an open environment. Our measurements showed a range of 2.14–3.44 depending on stage of canopy closure (manuscript in review). We set the eastern redcedar CANMAX as 2.0–4.0 mm. Juniper LAI usually varies between 0.91 and 5.2 (Owens, 2008) and we set the range of the eastern redcedar LAIs as 1–6. We used the Penman–Monteith equation to compute PET. At our site, the heights of individual eastern redcedar trees varied greatly; therefore, a wide range of 3–12 m was initially assigned as the maximum canopy height. Our wind speed was measured at 3 m above ground, and SWAT scaled the wind speed to the 1 m above the eastern redcedar canopy based on canopy height. Juniper is reported to be capable of producing very deep roots (Jackson et al., 1999), but the actual rooting depth is largely constrained by edaphic factors (Litvak et al., 2010). Our site is underlined by sandstone and shale so we set the range of rooting depth of 2–4 meters. Based on our measurements at the site (unpublished data), the range of stomatal conductance was set from 0.001 to 0.002 m/s.

Soil Conservation Service-Curve Number (SCS-CN) is used to partition surface runoff and water retention in the canopy and soil profile in this study. SCS-CN is the most important hydrological parameter. It is affected not only by the vegetation, but is also closely related to underlying soil hydraulic properties. Although we have multiple field sites, soil class only covers hydrologic soil groups B and D (soils with moderate and very slow infiltration rates, respectively). We inferred the SCS-CN number for hydrologic soil groups A and C proportionally according to the information for evergreen trees in SWAT default database. In addition, soil evaporation compensation factor (ESCO) and groundwater 'revap' coefficient were included for model calibration since they play considerable roles in impacting soil water budget and ET flux.

2.3. Model optimization

We optimized the SWAT model using both surface runoff and soil moisture data. Parameter compensation and non-uniqueness problems prevent the model auto-calibration algorithm from targeting reasonable and meaningful parameters that represent the watershed ecohydrological processes. Inclusion of multiple water and energy variable observations is an effective and widely used procedure to reduce model freedom and parameter uncertainty (Sorooshian and Gupta, 1983; Yapo et al., 1998; Gupta et al., 1999; Crow et al., 2003; van Griensven et al., 2006; Lo et al., 2010). In addition, the multiple paired watersheds used in this study can somewhat account for the spatial variability of hydrological processes due to soil and topography effects. Eq. (1) shows the objective function (F_{obj}) for model optimization, which includes two parts: one is the slope-scaled coefficient of determination (bR^2) and the other is Nash–Sutcliff coefficient (NSCE). Both indices are equal to one if simulation exactly fits the observation. These two indices are integrated to increase the likelihood to reduce both the system and random errors of simulations. Qiao et al. (2013a,b) suggested that the model optimized with least square error does not exactly correspond to the highest value of bR^2 and a balance point between them would point to a more superior model. Eq. (1) only shows the objective function for surface runoff and a similar equation also was used for the soil water storage difference between eastern redcedar encroached watersheds and grassland watersheds. We used the difference of water storage under contrasting vegetation covers rather than the absolute value to eliminate the system errors of the soil moisture monitoring sensor system in quantifying soil water content.

$$F_{\text{obj}} = \sum_{k=1}^{n} b_k R_k^2 + \sum_{k=1}^{n} 1 - \frac{\sum_{l=1}^{m} (q_{obs,n,l} - q_{sim,n,l})^2}{\sum_{l=1}^{m} (q_{obs,n,l} - \bar{q}_{obs,n})^2} \quad (1)$$

Table 1
Eastern redcedar biophysical and hydrological parameters in comparison to grassland.

		Eastern redcedar woodland			Grassland
		Best estimation	Minimum	Maximum	
Biophysical parameters (units)	CANMAX (mm)	3.17	2.0	4.0	1.8
	BLAI	4.98	1	6	2.5
	CHTMX (m)	7.27	3	12	1
	RDMX (m)	2.78	2	4	2
	GSI (m/s)	0.0016	0.001	0.002	0.005
Hydrological parameters	CN2-hydrologic (group A)	17.19	25	98	45.3
	CN2-hydrologic (group B)	37.82	25	98	63.8
	CN2-hydrologic (group C)	48.14	25	98	73.1
	CN2-hydrologic (group D)	52.95	25	98	77.7
	ESCO	0.53	0.5	1	0.97
	GW_REVAP	0.065	0.02	0.2	0.056

CANMAX (mm): Maximum Canopy Storage (mm)
BLAI: Max leaf area index
CHTMX (m): Max canopy height
RDMX (m): Max root depth
GSI (m/s): Max stomatal conductance (in drought condition)
CN2: SCS runoff curve number for moisture condition II
ESCO: Soil evaporation compensation factor
GW_REVAP: Groundwater "revap" coefficient

R^2 is coefficient of determination of observed and simulated surface runoff and b is slope of their linear regression. Surface runoff measurement and its mean are denoted as q and $\bar{q}$. Subscripts of *obs* and *sim* stand for observations and simulations. Denotations of n and m are the numbers of watershed and observation times for the variable.

With this objective function consisting of multiple hydrological variables measured from multiple watersheds, the SWAT model was optimized with the Shuffled complexes with Principal component analysis (SP-UCI) algorithm (Chu et al., 2010, 2011). The SP-UCI algorithm developed from the Shuffled Complexes Evolution (SCE_UA) (Duan et al., 1993, 1994) can prevent parameter population degradation and provide better parameter effectiveness in control of the uncertainty distribution. To our knowledge, this is a novel application of SP-UCI in SWAT model calibration.

3. Results

3.1. Calibration results

3.1.1. Simulations of PET and ET_a

The monthly simulations of PET and ET_a with the calibrated SWAT model are shown in Fig. 2. The calculated PET was constantly greater for the grassland mainly due to higher wind speed measurements in its open environment. Annual total PET, if accumulated from the monthly data, was generally higher than 1100 mm and less than 1300 mm on average from grassland and eastern redcedar encroached watersheds across the dry-to-wet year period. PET declined from 2011 to 2013, corresponding with the development of wetter and cooler atmospheric conditions.

Although PET was greater in the grassland watersheds, the ET_a was less than in the eastern redcedar encroached watersheds in each of the simulated three years. In contrast to the decreasing trend in PET, ET_a increased with the increase of precipitation from 2011 to 2013, in particular for the eastern redcedar encroached watersheds. For the driest year, 2011, ET_a was limited by the precipitation input for both types of land cover and therefore the difference in ET_a was negligible. In 2012, another drought year in the southern Great Plains, the ET_a was almost equal to the precipitation in the encroached watersheds while there were 100 mm potential water yield in the grassland. However, ET_a was less than the precipitation during spring, which potentially created chances for surface runoff generation in the encroached watersheds. 2013 was the wettest year of the period with annual precipitation of nearly 1000 mm, during which the monthly ET_a was constantly higher in the encroached watersheds, making a total difference of 200 mm between the two types of land cover. On average, evapotranspiration from the eastern redcedar encroached watersheds was annually 100 mm greater than from the grassland during the three years of dry-to-wet cycle.

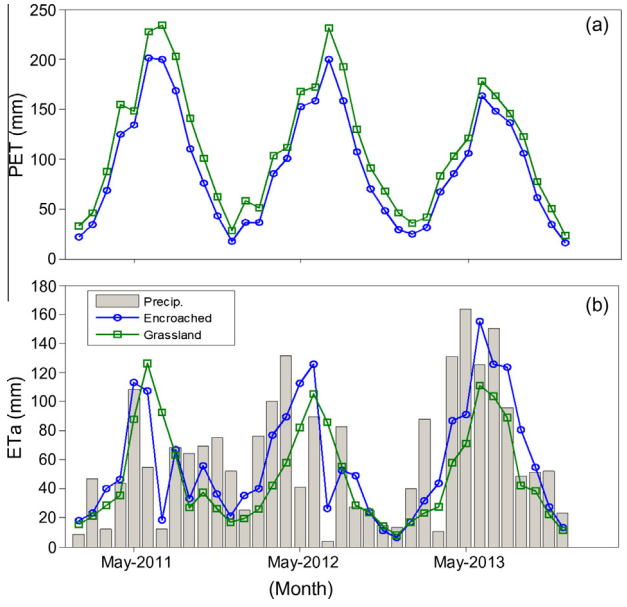

Fig. 2. The monthly PET (a) and actual ET (b) simulations for the grassland and eastern redcedar encroached watersheds.

3.1.2. Simulations of surface runoff and soil moisture

Fig. 3 shows the comparison of simulated and observed surface runoff on a monthly scale for the three pairs of grassland and eastern redcedar encroached watersheds as well as the mean for encroached and grassland watersheds. Observed surface runoff production either in peak flow or total amount was higher in grassland during the 3-year time period except for the exceptional dry year of 2011. The severe 2011 drought resulted in nearly zero runoff generation. In 2012 and 2013, the grassland watersheds had almost triple the surface runoff production when compared to the eastern redcedar encroached watersheds in either total amounts or peaks. Driven by the high precipitation in 2013, surface runoff increased significantly from the grassland watersheds; however, this was not the case for the eastern redcedar watersheds in which peak runoff was reduced in 2013 compared to 2012 even though precipitation increased. The highest monthly runoff occurred in April of 2012 and in May of 2013. Averaged across the watersheds, the highest monthly surface runoff depths were 29 mm and 31 mm for grassland watersheds and 13 mm and 8 mm for eastern redcedar encroached watersheds respectively for these two years.

The surface runoff simulations agreed very well to the observations for both grassland and eastern redcedar encroached watersheds (Fig. 3). The multi-site averaged simulation was the best after the model was optimized based on the multiple paired watersheds rather than any single one. Notably, the model represents well the vegetation effect on surface runoff under climate variability: an increasing pattern of surface runoff for the grassland but a decreasing pattern for the eastern redcedar woodland following the shifting of precipitation regime from 2012 to 2013. However, the calibrated model does show some performance difference with regards to the specific watersheds. For example, grassland watershed 1 had approximately 10 mm greater surface runoff than watersheds 2 and 3 and consequently its runoff peaks were underestimated following the multi-site mean optimization strategy. Peak runoff also was underestimated for the eastern redcedar encroached watersheds, e.g., watershed 4 for 2012 and 2013 and watershed 6 for 2012.

We evaluated the model performance upon a series of statistical indices (Table 2), which included coefficient of determination (R^2), slope-scaled coefficient of determination (bR^2), Nash–Sutcliff coefficient (NSCE), relative bias in percentage terms (Pbias) and normalized root mean square error (NRMSE). The NRMSE was also called RSR (ratio of root mean square error to the standard deviation of measured data) by Moriasi et al. (2007). The statistic values indicate that the model performed well not only on monthly scale but also on daily scale. The values of NSCE, R^2, and bR^2 at the daily scale were as high as 0.90, 0.90, and 0.85 for eastern redcedar watersheds and 0.96, 0.96, and 0.95 for grassland watersheds, respectively, showing slightly better simulations for the grassland watersheds. Overall, the model showed minor overestimation throughout the three years. The bias was greater in eastern redcedar encroached watersheds than grassland watersheds, 33% versus 11%. The larger overestimation in redcedar simulation is reasonable considering that the surface runoff generation is very low in

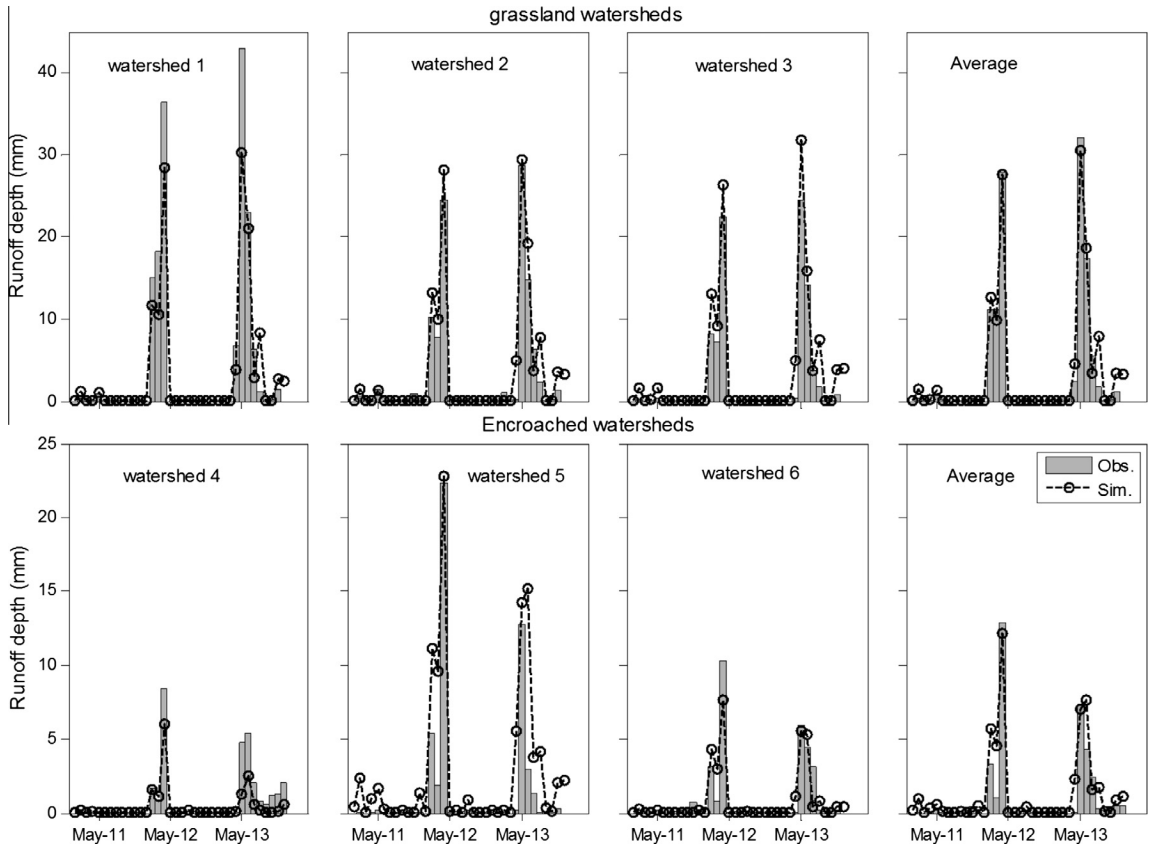

Fig. 3. Comparison of observed versus simulated monthly runoff depth from the grassland (upper panel, watersheds 1–3) and eastern redcedar encroached (lower panel, watersheds 4–6) watersheds.

Table 2
Statistical indices of hydrological simulations of the paired experimental watersheds (grassland and redcedar-encroached) and the mesoscale Council Creek watershed.

Statistic indices	Time scale	Average of encroached watersheds	Average of grassland watersheds	Mean of all experimental watersheds	Council Creek watershed
NSCE	Daily	0.90	0.96	0.93	0.40
	Monthly	0.84	0.97	0.91	0.79
R^2	Daily	0.90	0.96	0.93	0.67
	Monthly	0.87	0.97	0.92	0.90
bR^2	Daily	0.85	0.95	0.90	0.41
	Monthly	0.84	0.96	0.90	0.66
Pbias (%)	Daily	34	11	23	16
	Monthly	33	8	21	17
NRMSE	Daily	0.32	0.21	0.27	0.77
	Monthly	0.40	0.18	0.29	0.46

NSCE: Nash–Sutcliffe coefficient.
R^2: coefficient of determination.
bR^2: slope weighted coefficient of determination.
Pbias: percentage bias of simulation relative to observation.
NRMSE: normalized root mean square error.

the eastern redcedar encroached watersheds, usually less than 10 mm on a monthly basis during the wet season, such that a small absolute error results in a larger relative error.

Soil water storage anomalies, the soil moisture deviations from multiple-year average, are shown in Fig. 4. Due to the later installation of soil water content monitoring equipment, our observed soil moisture record is shorter than our surface runoff record. The observed soil water content was very low in the late months of 2012 and hit the lowest point at the end of that year. Observed soil moisture began to increase in January 2013 and continued to increase to well above the average until it peaked in June 2013 at a level that was 170 mm greater than the lowest point in December 2012. The amplitude of the anomalies was almost equal for both grassland and eastern redcedar encroached watersheds, suggesting that soil moisture holding capacity below the two vegetation types is similar (Zou et al., 2013). The model successfully tracks the soil moisture changes for both types of watersheds, including the abrupt dip in September and October 2013 and the rebound in November and December 2013. However, the soil moisture in the eastern redcedar encroached watersheds kept decreasing in the winter, again suggesting the higher water consumption by this evergreen species.

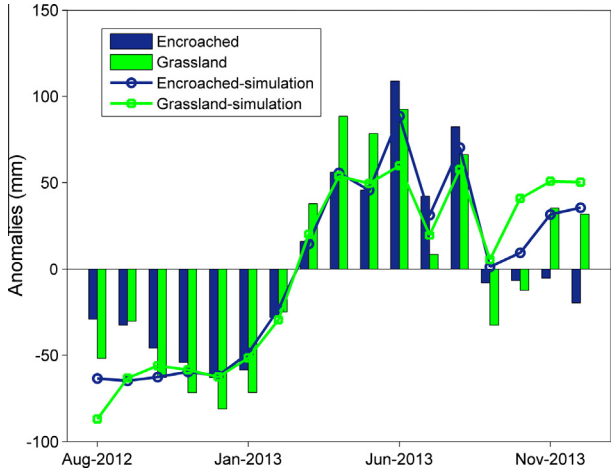

Fig. 4. Comparison of observed versus simulated soil water storage anomalies for the grassland and eastern redcedar encroached watersheds.

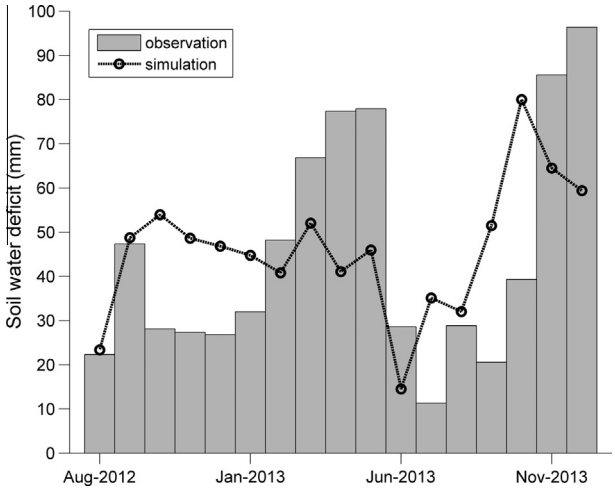

Fig. 5. Comparison of observed versus simulated soil water storage deficit, the difference of the grassland soil moisture storage and the eastern redcedar encroached soil moisture storage.

Although the soil moisture anomalies varied in the same pattern, the absolute soil moisture quantity in eastern redcedar encroached watersheds was consistently lower than that of the grassland watersheds. Soil moisture of the encroached watersheds subtracted from the soil moisture of grassland watersheds gives the difference or 'deficit' that could be attributed to the encroachment (Fig. 5). Small deficits in 2012 were due to the limited precipitation input and the resultant constant low soil moisture throughout the year. The soil moisture difference, however, was amplified in the wet year of 2013 and reached 80 mm in spring and 100 mm in December. As mentioned above, soil moisture recovered in winter in the grassland while it kept decreasing in eastern redcedar encroached watersheds. This suggests that eastern redcedars use more water relative to grasslands when water supply is ample. The soil water deficit in the eastern redcedar encroached watersheds also was well simulated with lower deficits in the drier year and higher deficits in the wetter year.

3.2. Validation in the Council Creek watershed

Model validation using Council Creek watershed data showed that the model calibrated to the experimental watersheds was capable of representing the hydrological process over a long historical time period and a larger spatial scale. The model not only reproduced the annual and monthly streamflow but also captured the peaks and recession of hydrography at the daily time scale for the Council Creek watershed (Fig. 6). Compared to the simulations for the experimental watersheds, the model performance at Council Creek watershed was not as accurate and the statistical values indicated lower correspondence to observed values, but they were still competitive (Table 2). NSCE was 0.40 and 0.79, R^2 was 0.67 and 0.90, and bR^2 was 0.41 and 0.66, at the daily and monthly scales respectively for each index.

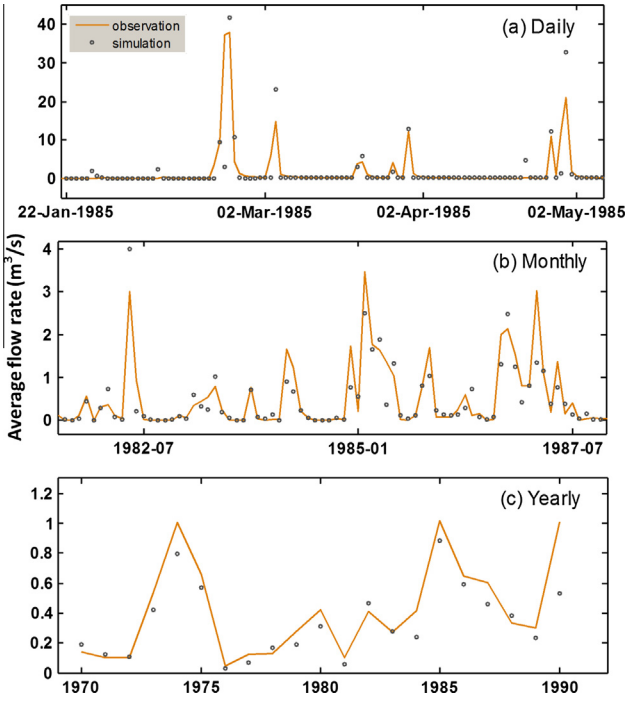

Fig. 6. Model validation in a larger scale watershed - Council Creek watershed: (a) daily, (b) monthly, and (c) yearly scales of streamflow observation and simulation from 1970 to 1990.

4. Discussion

Evapotranspiration is the prevailing component of the water budget in water-limited rangelands. The challenge of model simulation for such systems is to improve estimation of PET and ET_a. Our results showed that the PET was higher for grassland due largely to the higher wind speed measurements in the grassland. The grassland has shorter vegetation (mostly < 1 m) and lacks the canopy roughness of the redcedar woodland such that the grassland usually had wind speed twice that in the eastern redcedar when measured at the 3-m height. Therefore calculation of PET is subject to large uncertainty if meteorological forcing is limited. Uncertainty of PET could magnify through the process and increase the uncertainty of ET_a. Incorporation of soil moisture into the process in our study was able to confine the error propagation.

The performance of the calibrated model in the larger watershed was less accurate than in the small experimental watersheds and the statistical values were also degraded. We attribute this largely to inadequate information of climate forcing. For the large watershed, rainfall and weather measurements are not as precise as those of the experimental watersheds which have weather stations at the exact locations. There is only one available weather station located within the Council Creek watershed and that is at the southernmost portion (Fig. 1). This one station may

not be representative enough considering the spatial variability of rainfall, especially the warm-season convective rainfall contribution in this region (Ruiz-Barradas and Nigam, 2005; Qiao et al., 2014a). The high rainfall spatial variability during storm events for the nearby intermediate to large watersheds can be seen from the study of Qiao et al. (2014b). However, the percent bias is improved to 16%, compared to 23% for the experimental watersheds due to the large streamflow quantities produced by the large landscape watershed.

Due to lack of parameters for juniper species, pine growing in forests are often used as initial model inputs. However, recent studies emphasized differences in both ecophysiological characteristics and soil physical and hydrological properties associated with woody encroachment compared to forests. Although juniper trees are usually shorter than pine trees, the canopy interception of juniper can be 2–3 mm higher than any other species in the region including the oak trees (Owens et al., 2006; Starks et al., 2014). The stomatal conductance was set at 0.001–0.002 m/s based on field measurement by Will et al. (unpublished data), which is lower than pine trees that are typically 0.002 m/s.

Previous studies mostly focused on intermediate sized watersheds at scales of 10–10^2 km^2 and relied solely on historic streamflow data to calibrate the model (e.g., Bednarz et al., 2000; Brown and Raines, 2002; Afinowicz et al., 2005; Harmel et al., 2006). The streamflow from watersheds at this scale is usually composed of surface runoff and baseflow. Inclusion of baseflow is likely to cause disproportional or even opposite contributions of surface runoff and subsurface runoff due to parameter compensation in simulations if only streamflow is optimally calibrated. Arguably, it is more difficult to constrain the water budget or hydrological signatures at this scale, as spatial variability of rainfall and soil moisture play roles in biasing water balance and partitioning among water flux and storages. In comparison, previous simulations in juniper watersheds had much lower performance either in calibration or validation; e.g., the NSCE of monthly simulation was 0.79 in this study compared to 0.5 or less in the study of Afinowicz et al. (2005) for the mesoscale watersheds.

Multiple comprehensive paired experimental watersheds at single digit hectare scale are seldom designed to comparatively study woody encroachment impacts on hydrology. For these enclosed small watersheds, the flumes can maximally measure the surface runoff or overland flow. This is very helpful to determine parameters related to rainfall and runoff processes, such as the SCS-CN values, which are very important parameters in SWAT modeling. The addition of the soil water component is vital in controlling water balance and modeling freedom toward a proper partitioning of the ET component. Synchronous measurement increases the resolution to compare the hydrological effect on grassland and eastern redcedar encroached watersheds under the same climatic condition, either dry or wet. Another important factor is that woody plant encroachment tends to be patchy in the southern Great Plains, and larger paired watersheds contain multiple types of vegetation cover and thus the ability to directly compare contrasting vegetation types could be lost.

The ecohydrological community has being making progress in untangling carbon and water coupling associated with woody encroachment through modeling approaches. Most recently, O'Donnell and Caylor (2012) modeled the changes in soil water and carbon stock after woody plant encroachment across different climate zones of the western United States. Pierini et al. (2014) parameterized the Triangulated Irregular Network-based Real-time Integrated Basin Simulator (tRIBS) model to investigate the mechanism of surface runoff reduction associated with mesquite (*Prosopis velutina*) encroachment in the Sonoran Desert. Calibration of existing models using experimental watershed observations as we demonstrated for the SWAT model could largely reduce model uncertainty for predicting the impact of invasive and/or encroaching species on ecosystem goods and services under prevailing climate change scenarios for water-limited rangeland.

5. Summary and conclusion

This study strived to physically parameterize a regionally important encroaching species (eastern redcedar) in the SWAT model using comprehensive *in-situ* measurements from three paired experimental watersheds in the south-central Great Plains, USA. The small scale experimental watersheds provided accurate water balance control with respect to the rainfall, runoff and soil water storage variations. The recently developed SP-UCI algorithm was used to evolutionarily search the best biophysical and hydrological parameters of the juniper within proper initial ranges. The results of the calibrated SWAT model are very encouraging in simulation of the hydrological processes for three pairs of grassland and eastern redcedar encroached watersheds. Specifically, the model successfully reproduced the consistently low soil moisture and surface runoff from eastern redcedar encroached watersheds during the 3-year monitoring period. Modeling results suggest a strong climate dependency of ET difference between the grassland and eastern redcedar encroached watersheds from zero in the drought year (2011) to as much as 200 mm in the exceptional wet year (2013). The calibrated SWAT model adequately simulated the long-term streamflow of a nearby, larger watershed under rapid eastern redcedar encroachment since 1970. To our knowledge, this is the first complete set of biophysical and hydrological parameters for juniper species.

Substantial uncertainties exist in terms of the impact of woody plant invasion and encroachment into rangeland on ecosystem goods and services, especially under the increasing climate variability. Model calibration using *in situ* observations resulted in substantial improvement in simulation at the landscape scale. Calibration of existing, physically based transport models or model frameworks with highly controlled observations such as experimental watershed data is critical to reduce the uncertainty of hydrological models in simulation for woody encroachment. Results from those improved model simulation can provide actionable recommendation for climate change adaptation and mitigation at landscape and river basin scales.

Acknowledgements

Dr. Lei Qiao is a postdoctoral associate supported by USGS South-central Climate Science Center and the Oklahoma Agricultural Experiment Station. This study was also supported with funding from NSF EPSCoR (NSF-1301789), NSF Dynamics of Coupled Natural and Human Systems (CNH) program (DEB-1413900) and USDA National Institute of Food and Agriculture AFRI Sustainable Bioenergy program (2014-67010-21653).

References

Afinowicz, J., Munster, C., Wilcox, B., 2005. Modeling effects of brush management on the rangeland water budget: Edwards Plateau, Texas. J. Am. Water Resour. Assoc. 41, 181–193.

Archer, S., Schimel, D., Holland, E., 1995. Mechanisms of shrubland expansion: land use, climate or CO2? Climatic Change 29, 91–99.

Arnold, J., Srinivasan, R., Muttiah, R., Williams, J., 1998. Large area hydrologic modeling and assessment Part I: model development. J. Am. Water Resour. Assoc. 34, 73–89.

Arnold, J., Moriasi, D., Gassman, P., Abbaspour, K., White, M., Srinivasan, R., Santhi, C., Harmel, R., Van Griensven, A., Van Liew, W., Kannan, N., Jha, M., 2012. SWAT: model use, calibration, and validation. Trans. ASABE 55, 1491–1508.

Bednarz, S., Dybala, T., Muttiah, R., Rosenthal, W., Dugas, W., 2000. Brush Management/water Yield Feasibility Studies for Eight Watersheds in Texas – TR-182. Texas Water Resources Institute, College Station, Texas.

Briggs, J., Knapp, A., 1995. Interannual variability in primary production in tallgrass prairie: climate, soil moisture, topographic position, and fire as determinants of aboveground biomass. Am. J. Bot. 82, 1024–1030.
Briggs, J., Knapp, A., Blair, J., Heisler, J., Hoch, G., Lett, M., McCarron, J., 2005. An ecosystem in transition: causes and consequences of the conversion of mesic grassland to shrubland. Bioscience 55, 243–254.
Brown, D., Raines, T., 2002. Simulation of flow and effects of Best Management Practices in the upper Seco Creek Basin, south-central Texas, 1991–98, Water-Resources Investigations Report 02-4249, U.S. Geological Survey, Austin, Texas.
Bumgarner, J., Thompson, F., 2012. Simulation of streamflow and the effects of brush management on water yields in the upper Guadalupe River Watershed, South-central Texas, 1995–2010, Scientific Investigations Report 2012-5051, U.S. Geological Survey, Reston, Virginia.
Caterina, G., Will, R., Turton, D., Wilson, D., Zou, C., 2014. Water use of *Juniperus virginiana* trees encroached into mesic prairies in Oklahoma, USA. Ecohydrology 7, 1124–1134.
Chu, W., Gao, X., Sorooshian, S., 2010. Improving the shuffled complex evolution scheme for optimization of complex nonlinear hydrological systems: application to the calibration of the Sacramento soil-moisture accounting model. Water Resour. Res. 46, W09530.
Chu, W., Gao, X., Sorooshian, S., 2011. A solution to the crucial problem of population degeneration in high-dimensional evolutionary optimization. Syst. J., IEEE 5, 362–373.
Crow, W., Wood, E., Pan, M., 2003. Multiobjective calibration of land surface model evapotranspiration predictions using streamflow observations and spaceborne surface radiometric temperature retrievals. J. Geophys. Res. 108, 4725.
Duan, Q., Gupta, H., Sorooshian, S., 1993. Shuffled complex evolution approach for effective and efficient global minimization. J. Optim. Theory Appl. 76, 501–521.
Duan, Q., Sorooshian, S., Gupta, V., 1994. Optimal use of the SCE-UA global optimization method for calibrating watershed models. J. Hydrol. 158, 265–284.
Dugas, W., Hicks, R., Wright, P., 1998. Effect of removal of *Juniperus ashei* on evapotranspiration and runoff in the Seco Creek Watershed. Water Resour. Res. 34, 1499–1506.
Engle, D., Coppedge, B., Fuhlendorf, S., 2008. From the dust bowl to the green glacier: human activity and environmental change in Great Plains grasslands. In: van Auken, O.W. (Ed.), Western North American Juniperus Communities. Springer, New York, pp. 253–271.
Gupta, H., Bastidas, L., Sorooshian, S., Shuttleworth, W., Yang, Z., 1999. Parameter estimation of a land surface scheme using multicriteria methods. J. Geophys. Res. 104, 19491–19503.
Harmel, R., Cooper, R., Slade, R., Haney, R., Arnold, J., 2006. Cumulative uncertainty in measured streamflow and water quality data for small watersheds. Trans. ASABE 49, 689.
Holtan, H.N., Minshall, N.E., Harrold, L.L., 1962. Field manual for research in agricultural hydrology, Soil and Water Conservation Research Division, Agricultural Handbook No. 224, U.S. Department of Agriculture, Washington, D.C.
Houghton, R., Hackler, J., Lawrence, K., 1999. The U.S. carbon budget: contributions from land-use change. Science 285, 574–578.
Huang, Y., Wilcox, B., Stern, L., Perotto-Baldivieso, H., 2006. Springs on rangelands: runoff dynamics and influence of woody plant cover. Hydrol. Process. 20, 3277–3288.
Huxman, T., Wilcox, B., Breshears, D., Scott, R., Snyder, K., Small, E., Hultine, K., Pockman, W., Jackson, R., 2005. Ecohydrological implications of woody plant encroachment. Ecology 86, 308–319.
Archer, S., Scifres, C., Bassham, C., Maggio, R., 1988. Autogenic succession in a sub-tropical savanna – conversion of grassland to thorn woodland. Ecol. Monogr. 58, 111–127.
Jackson, R., Moore, L., Hoffmann, W., Pockman, W., Linde, r.C., 1999. Ecosystem rooting depth determined with caves and DNA. Proc. Natl. Acad. Sci. 96, 11387–11392.
Litvak, E., Susan, S., James, H., 2010. Woody plant rooting depth and ecosystem function of savannas: a case study from the Edwards Plateau Karst, Texas. In: Hill, M., Hanan, N. (Eds.), Ecosystem Function in Savannas: Measurement and Modeling at Landscape to Global Scales. CRC Press, pp. 17–134.
Liu, W., Hong, Y., Khan, S., Huang, M., Vieux, B., Caliskan, S., Grout, T., 2010. Actual evapotranspiration estimation for different land use and land cover in urban regions using Landsat 5 data. J. Appl. Remote Sens. 4, 041873.
Lo, M.-H., Famiglietti, J., Yeh, P., Syed, T., 2010. Improving parameter estimation and water table depth simulation in a land surface model using GRACE water storage and estimated base flow data. Water Resour. Res. 46, W05517.
McCole, A., Stern, L., 2007. Seasonal water use patterns of *Juniperus ashei* on the Edwards Plateau, Texas, based on stable isotopes in water. J. Hydrol. 342, 238–248.
Moriasi, D., Arnold, J., Van Liew, M., Bingner, R., Harmel, R., Veith, T., 2007. Model evaluation guidelines for systematic quantification of accuracy in watershed simulations. Trans. ASABE 50, 885–900.
Newman, B., Wilcox, B., Archer, S., Breshears, D., Dahm, C., Duffy, C., McDowell, N., Phillips, F., Scanlon, B., Vivoni, E., 2006. Ecohydrology of water-limited environments: a scientific vision. Water Resour. Res. 42, W06302.
Norris, M., Blair, J., Johnson, L., McKane, R., 2001. Assessing changes in biomass, productivity, and C and N stores following *Juniperus virginiana* forest expansion into tallgrass prairie. Canada J. Forest Res. 31, 1940–1946.
O'Donnell, F., Caylor, K., 2012. A model-based evaluation of woody plant encroachment effects on coupled carbon and water cycles. J. Geophys. Res.: Biogeosci. 117, G02012.
Owens, K., 2008. Juniper tree impacts on local water budgets. In: van Auken, O.W. (Ed.), Western North American Juniperus Communities. Springer, New York, pp. 188–201.
Owens, K., Lyons, R., Alejandro, C., 2006. Rainfall partitioning within semiarid juniper communities: effects of event size and canopy cover. Hydrol. Process. 20, 3179–3189.
Pierini, N., Vivoni, E., Robles-Morua, A., Scott, R., Nearing, M., 2014. Using observations and a distributed hydrologic model to explore runoff thresholds linked with mesquite encroachment in the Sonoran Desert. Water Resour. Res. 50, 8191–8215.
Qiao, L., Herrmann, R., Pan, Z., 2013a. Parameter uncertainty reduction for SWAT using GRACE, streamflow, and groundwater table data for lower Missouri River Basin. J. Am. Water Resour. Assoc. 49, 343–358.
Qiao, L., Pan, Z., Herrmann, R., Hong, Y., 2013b. Hydrological variability and uncertainty of Lower Missouri River Basin under changing climate. J. Am. Water Resour. Assoc. 50, 246–260.
Qiao, L., Hong, Y., McPherson, R., Shafer, M., Gade, D., Williams, D., Chen, S., Lilly, D., 2014a. Climate change and hydrological response in the trans-state Oologah Lake watershed–evaluating dynamically downscaled NARCCAP and statistically downscaled CMIP3 simulations with VIC model. Water Resour. Manage 28, 3291–3305.
Qiao, L., Hong, Y., Chen, S., Zou, C.B., Gourley, J.J., Yong, B., 2014b. Performance assessment of the successive Version 6 and Version 7 TMPA products over the climate-transitional zone in the southern Great Plains, USA. J. Hydrol. 513, 446–456.
Ratajczak, Z., Nippert, J., Collins, S., 2011. Woody encroachment decreases diversity across North American grasslands and savannas. Ecology 93, 697–703.
Ruiz-Barradas, A., Nigam, S., 2005. Warm season rainfall variability over the U.S. Great Plains in observations, NCEP and ERA-40 reanalyses, and NCAR and NASA atmospheric model simulations. J. Clim. 18, 1808–1830.
Schimel, D., House, J., Hibbard, K., Bousquet, P., Ciais, P., Peylin, P., Braswell, B., Apps, M., Baker, D., Bondeau, A., Canadell, J., Churkina, G., Cramer, W., Denning, A., Field, C., Friedlingstein, P., Goodale, C., Heimann, M., Houghton, R., Melillo, J., Moore, B., Murdiyarso, D., Noble, I., Pacala, S., Prentice, I., Raupach, M., Rayner, P., Scholes, R., Steffen, W., Wirth, C., 2001. Recent patterns and mechanisms of carbon exchange by terrestrial ecosystems. Nature 414, 169–172.
Soil Conservation Service, 1987. Soil Survey of Payne County, Oklahoma, USDA, Washington, D.C.
Sorooshian, S., Gupta, V., 1983. Automatic calibration of conceptual rainfall-runoff models: the question of parameter observability and uniqueness. Water Resour. Res. 19, 260–268.
Starks, J., Venuto, B., Dugas, W., Kiniry, J., 2014. Measurements of canopy interception and transpiration of openly-grown eastern redcedar in central Oklahoma. Environ. Nat. Resour. Res. 4, 103–122.
Stoeser, D., 2005. Preliminary integrated geologic map databases for the United States: Central states, Montana, Wyoming, Colorado, New Mexico, Kansas, Oklahoma, Texas, Missouri, Arkansas, and Louisiana, USGS, Reston, Virginia.
van Griensven, A., Meixner, T., Grunwald, S., Bishop, T., Diluzio, M., Srinivasan, R., 2006. A global sensitivity analysis tool for the parameters of multi-variable catchment models. J. Hydrol. 324, 10–23.
Wilcox, B., 2007. Does rangeland degradation have implications for global streamflow? Hydrol. Process. 21, 2961–2964.
Wine, M., Zou, C., 2012. Long-term streamflow relations with riparian gallery forest expansion into tallgrass prairie in the Southern Great Plains, USA. For. Ecol. Manage. 266, 170–179.
Wine, M., Ochsner, T., Sutradhar, A., Pepin, R., 2011. Effects of eastern redcedar encroachment on soil hydraulic properties along oklahoma's grassland-forest ecotone. Hydrol. Process. 26, 1720–1728.
Wu, X., Redeker, E., Thurow, T., 2001. Vegetation and water yield dynamics in an Edwards Plateau watershed. J. Range Manag. 54, 98–105.
Yapo, P., Gupta, H., Sorooshian, S., 1998. Multi-objective global optimization for hydrologic models. J. Hydrol. 204, 83–97.
Zou, C., Turton, D., Will, R., Engle, D., Fuhlendorf, S., 2013. Alteration of hydrological processes and streamflow with juniper (*Juniperus virginiana*) encroachment in a mesic grassland catchment. Hydrol. Process. 28, 6173–6182.